Dielectric Resonator Antenna With Enhanced Gain And Bandwidth For 5G Application

Prof. Lalitha N [1], Nandan U [2], Sohan Jain T B [3], Shreyank R [4], Sowndarya [5]

[2,3,4,5] Student, Department of Electronics and Communication Engineering, Vidya Vikas Institute of Engineering & Technology, Mysuru.

Abstract: In this paper, dielectric resonator antenna (DRA) with high gain and wide impedance bandwidth for fifth-generation (5G) wireless communication applications. The DRA is designed to operate at higher-order TEx15δ mode to achieve high antenna gain, while a hollow cylinder at the center of the DRA is introduced to improve bandwidth by reducing the quality factor. The DRA is excited by a microstrip line with a narrow aperture slot. The reflection coefficient, antenna gain, and radiation pattern of the proposed DRAs are analysed using the commercially available full-wave electromagnetic simulation tool CST Microwave Studio (CST MWS). The proposed antenna structures were fabricated and experimentally validated. Measured results of the fabricated prototypes show a 10-dB return loss impedance bandwidth of 10.7% (14.3–15.9 GHz) and 16.1% (14.1–16.5 GHz) for DRA1 and DRA2, respectively, at the operating frequency of 15 GHz. The results show that the designed antenna structure can be used in the Internet of things (IoT) for device-to-device (D2D) communication in 5G systems.

Keywords: *Dielectric resonator antenna, Higher-order mode, Quality factor, Gain, Bandwidth, 5G communication.*

1. Introduction

The presumptions and challenges of the ever-growing traffic explosion drew increased attention toward the significant research activity and development of fifth-generation (5G) wireless communication technology. The most effective way to fulfil the needs of the 5G communication system, which is expected to be launched commercially around 2020 and beyond, is to increase bandwidth. Thus, the migration to a higher-frequency band is essential to support the required high data rate on the order of gigabits per second (Gbps). However, the main problem associated with a higher-frequency band is the high path loss with short distance communication due to the short wavelengths. To overcome these issues, high-gain antennas are required to solve the problems of high path loss and increase the transmission range related to the high-frequency band. This method has distinct benefits compared to other gain enhancement techniques because it demonstrates high gain and requires a small area with a simple structure, which are attractive features for modern communication systems. However, this approach has the main problem of narrow impedance bandwidth. The gain of a rectangular DRA was enhanced by integrating it with a surface-mounted short horn (SMSH). The major drawback of this approach is the higher complexity, with increased size. Modification of the shape of the dielectric resonator was suggested to enhance the antenna gain. Recently, the higher-order mode technique has been adopted to enhance the gain of DRAs. A microstrip patch antenna (MSA) is considered as a good choice for 5G wireless communication due to its compact size, light weight, low cost, and ease of fabrication. However, at higher frequencies, the microstrip patch antenna suffers from low radiation efficiency because of the inherent metallic losses. Moreover, it offers low gain and narrow bandwidth. In contrast, dielectric resonator antennas (DRAs) exhibit higher radiation efficiency even at higher frequencies due to the absence of intrinsic conductor loss and surface wave loss. Dielectric resonator antennas, because of their numerous advantages and attractive features like light weight, low cost, and relatively wide impedance bandwidth, gained increased attention from antenna designers as a good candidate for 5G wireless communication. Additionally, they offer flexible excitation schemes such as coaxial feed probes, microstrip feed lines, aperture coupling, and co-planar waveguides.

2. Antenna Design and Analysis

The configuration of the proposed DRAs with dimensions of length (a), width (b), and height (d) is shown in figure 1 a, b operating at 15 GHz. The length, width, and height of the designed structure are represented as

$$a \times b \times d = 0.2\,\lambda \times 0.2\,\lambda \times 1\,\lambda$$

The DRA is made of an ECCOS-TOCK HiK material with a dielectric constant (εr) of 10 and loss tangent ($\tan\delta$) of 0.002. The Rogers™ RT/Duroid 5880 substrate with a permittivity of 2.2 and a loss tangent ($\tan\delta$) of 0.0009 is used. The thickness of the Rogers substrate is 0.254 mm. Each DRA is mounted on a

$$20\,mm \times 20\,mm = 1\lambda \times 1\lambda\ 20$$

ground plane and excited by a 50 Ω standard microstrip line with an aperture slot in the ground plane. The ground plane is printed on the top side of the substrate.

It is important to mention here that a microstrip feedline is used due to the ease of fabrication. The slot length l_s, width w_s and stub length S are adjusted to match individual antennas.

All dimensions are in millimetres(mm).In each case, stub length S was adjusted to optimize the matching impedance of individual DRAs.

The resonant frequencies, f_0, of the TExδnm mode can be predicted using a dielectric waveguide model (DWM).

The wave numbers k_x, k_y,and k_z can be deduced by solving the following transcendental equations:

$$k_x \tan\left(\frac{kxa}{2}\right) = \sqrt{(\varepsilon r - 1)ko2 - kx2} \text{------(1)}$$

$$k_x^2 + k_y^2 + k_z^2 = \varepsilon r ko2, \text{-------(2)}$$

where

$$k_o = \frac{2\pi fo}{a}, k_y = \frac{m\pi}{b}, k_z = \frac{n\pi}{c} \text{-------(3)}$$

$$f_o = \frac{c}{2\pi\sqrt{(\varepsilon r)}}\sqrt{\varepsilon r ko2} \text{ ------(4)}$$

where c is the velocity of light, εr is the relative permittivity of the DRA is the free space wave number, and m and n are half-wave field variations along directions, respectively. The symbols kx, ky,and kz represent the wave numbers in the x-, y-, and z-directions, respectively.

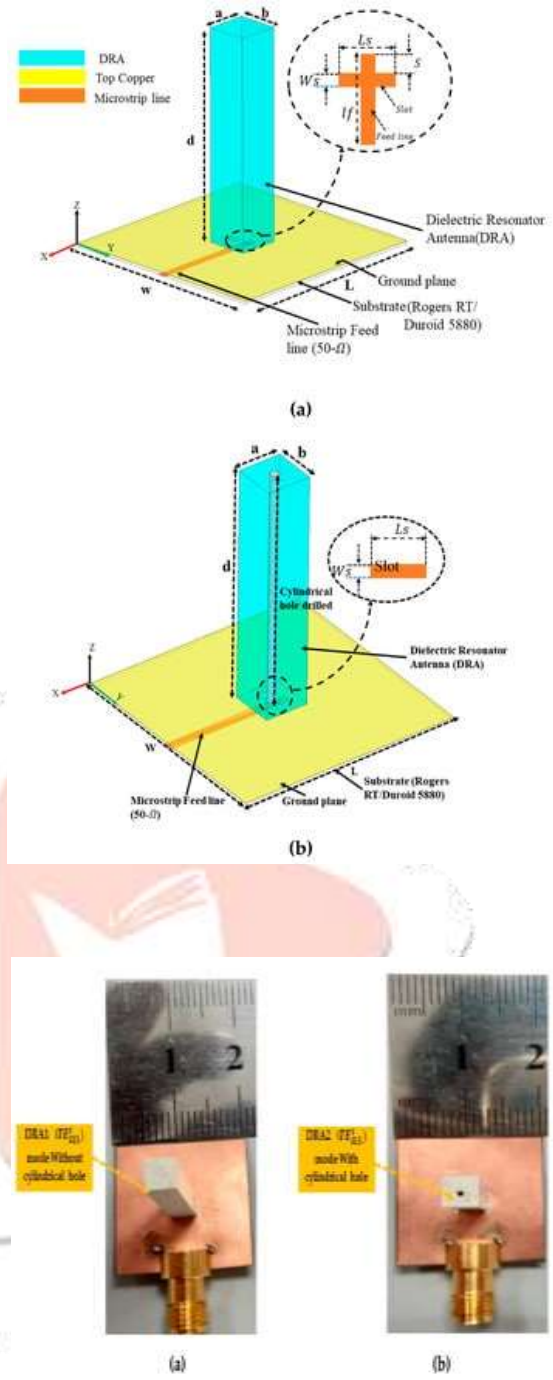

Figure 1. Configuration of the proposed dielectric resonator antennas (DRAs): (**a**) $TE\delta 15$ mode without cylindrical hole (DRA1); (**b**) $TE\delta 15$ mode with a cylindrical hole (DRA2).

Figure 2 compares the simulated reflection coefficients $|S_{11}|$of the DRA operating in higher-order ($TE\delta 15x$) mode without a cylindrical hole (DRA1) and that of the DRA with a cylindrical hole (DRA2). It can be seen from Figure 2 that the DRA operating in higher-order $TE\delta 15x$ mode without a cylindrical hole obtained an impedance bandwidth of 1.6 GHz (10.6%), ranging from 14.3 GHz to 15.9 GHz. The DRA operating in higher-order mode $TE\delta 15x$ with a cylindrical hole at the center achieved a comparatively wider impedance bandwidth of 2.6 GHz (17.4%), operating from 14.3

GHz to 16.9 GHz. The bandwidth of DRA2 was relatively larger than DRA1 because a hollow cylindrical hole was drilled at the center of the DRA2, which reduced the radiation Q-factor of the antenna; therefore, the impedance bandwidth was enhanced. Figure 3 a,b present the electric field (E-field) distribution in the *XY* plane for DRA1 (without a cylindrical hole) and DRA2 (with a cylindrical hole), respectively. The electric field distribution was stronger in DRA2 compared to DRA1. The cylindrical hole at the center of DRA2 strengthened the electric field near the center of the DRAs. This helped in increasing the bandwidth and efficiency of the DRAs. The simulated magnetic fields (H-fields) of both antennas are plotted in Figure 3 a,b, respectively, at the operating frequency of 15 GHz. Figure 4 a,b show the magnetic field distribution in higher-order ($T\ E\ x\ \delta$ 15) mode.

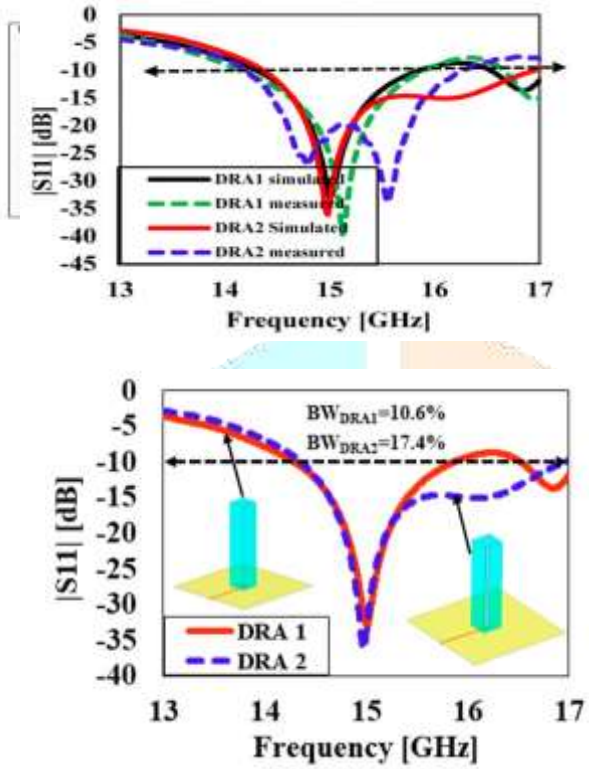

Figure 2. Simulated reflection coefficients $|S_{11}|$ of the proposed DRAs.

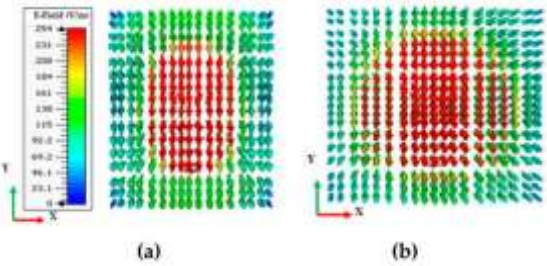

Figure 3. Simulated electric fields (E-fields) of the proposed DRAs at 15 GHz: (**a**) DRA1; (**b**) DRA2.

Figure 4. Simulated magnetic fields (H-fields) of the proposed DRAs at 15 GHz: (**a**) DRA1; (**b**) DRA2.

3. Measurement Results and Discussion

We observe and analyse the simulation and measured results. The performance of the antenna prototypes was designed and simulated using the commercial three-dimensional (3D) electromagnetic (EM) Computer Simulation Technology (CST) Microwave Studio software. The photographs of the fabricated proposed DR antennas are shown in Figure 5. The reflection coefficients were measured using a vector network analyser (VNA), while antenna gain and the radiation patterns were measured in an anechoic chamber. The simulated and measured results of reflection coefficients S_{11} of the DRA prototypes are depicted in Figure 6. It can be seen from Figure 6 that DRA1 obtained a simulated and measured −10-dB impedance bandwidth of 10.6% and 10.7%, respectively. On the other hand, DRA2 achieved a simulated and measured −10-dB bandwidth of 17.4% and 16.1%, respectively. The slight difference between the simulated and measured results can be attributed to fabrication imperfections.

Figure 5. Photos of the fabricated proposed antenna prototypes: (**a**) DRA1 without cylindrical hole (three-dimensional (3D) view); (**b**) DRA2 with cylindrical hole (3D view); (**c**) top view without DRA; (**d**) back view.

Figure 6. Simulated and measured reflection coefficients |S11| of DRA1 and DRA2.

3.1. T E x δ 15 *without Cylindrical Hole (DRA1)*

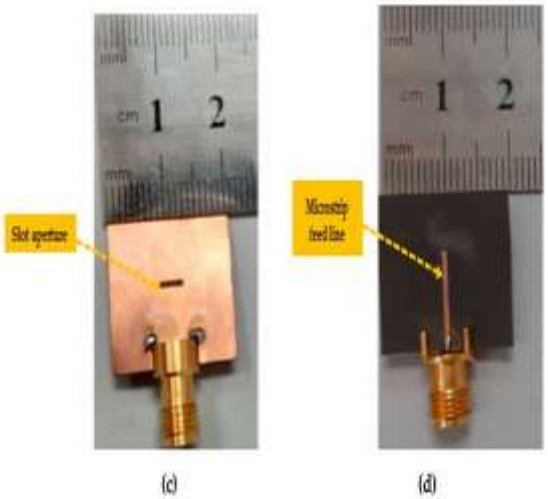

The simulated and measured reflection coefficients versus frequency plots of the $TE\,x\,\delta$ 15mode without a cylindrical hole (DRA1) are represented in Figure 7**.** It can be seen from Figure **7** that the proposed antenna attained simulated and measured −10-dB impedance bandwidths of 10.6% and 10.7%, respectively. The plot of the simulated and measured antenna gains and radiation efficiency as a function of frequency is depicted in Figure 8**.** With reference to the plot, the simulated and measured antenna gains were 10.5 dBi and 10.4 dBi, respectively. As presented in Figure 8, the measured and simulated radiation efficiencies were 97% and 95%, respectively.

Figure 7. Simulated and measured results of the reflection coefficient $|S_{11}|$ of DRA1.

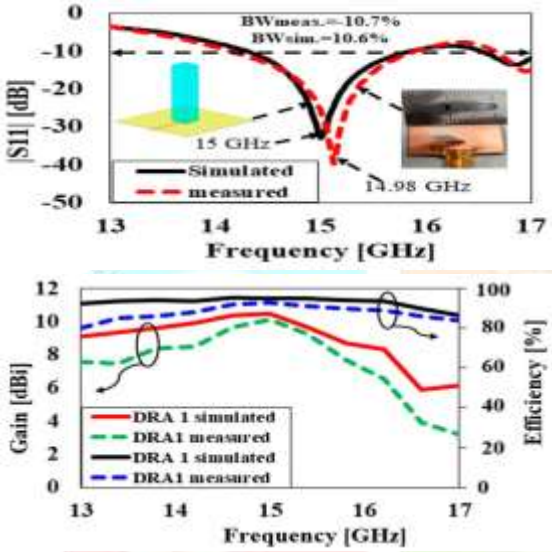

Figure 8. Simulated and measured gain and efficiency versus frequency of DRA1 at 15 GHz.

Figure 9 shows the simulated and measured normalized radiation pattern of the proposed structure in the E- and H-planes at 15 GHz. Figure 9 shows the normalized radiation pattern for DRA1 along the H-plane where the half-power beam width was 49.2∘49.2° in the major lobe and the radiated power in the side lobe level was −11.8dB. The major lobe is located at 0∘0°. In the E-plane, the half-power beam width in the major lobe was 46.4∘46.4° and the radiated power in the side lobe level was −9.3db.

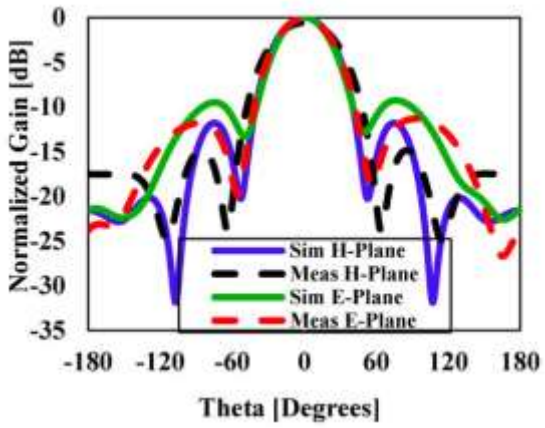

Figure 9. Simulated and measured normalized radiation pattern in the E-plane and H-plane of DRA1 at 15 GHz.

3.2. $TE\,x\,\delta$ **15** *with Cylindrical Hole (DRA2)*

Figure 10 demonstrates the simulated and measured reflection coefficients of the proposed antenna. With reference to Figure 10, the proposed antenna structure achieved simulated and measured bandwidths (S11<−10) of 17.4% (14.3–16.9 GHz) and 16.1% (14.1–16.5GHz), respectively. The slight difference in the measured and simulated results occurred because of the fabrication of the DRA during its assembly process Figure 11 shows the simulated and measured gain and efficiency of DRA2. It can be seen from Figure 11 that the simulated and measured antenna gains were 10.5 dBi and 10.4 dBi, respectively, while the simulated and measured radiation efficiencies were 98% and 96%, respectively. Figure 12 shows the simulated and measured normalized radiation pattern of DRA2 in the E-plane and H-plane at 15 GHz. Figure 12 shows the normalized radiation pattern for DRA2 with a cylindrical hole along the H-plane, where the half-power beam width was 54.1° in the major lobe, and radiated power in the side lobe level was −13.6 db. In the E-plane, the half-power beam width in major lobe was 48.6°, and the radiated power in the side lobe level was -10.4dB. The major lobe was located at 0°.

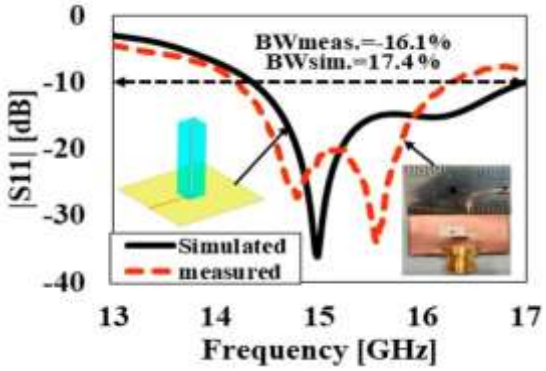

Figure 10. Simulated and measured results of the reflection coefficient $|S_{11}|$ of DRA2.

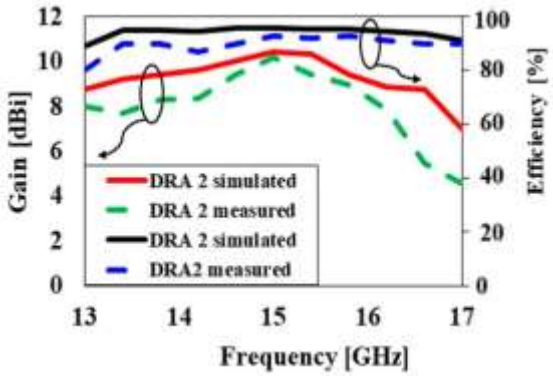

Figure 11. The simulated and measured antenna gain and radiation efficiency versus frequency of DRA2.

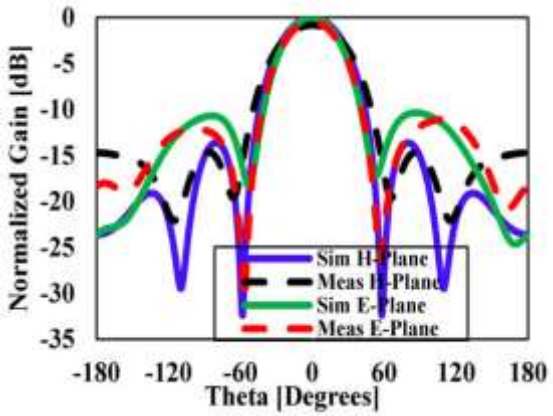

Figure 12. Simulated and measured normalized radiation pattern in the E-plane and H-plane of DRA2 at 15 GHz.

4. Evaluation of performance and outcomes in real-world use cases

The evaluation of 5G application performance and outcomes in real-world use cases is an ongoing process, and results can vary based on factors such as network deployment, location, and specific applications. Here's an assessment of 5G's performance and outcomes in several real-world use cases**:**

a. Enhanced Mobile Broadband (eMBB++):

- Performance: 5G provides significantly faster download and upload speeds compared to 4G, making it ideal for high-quality video streaming and large file downloads.
- Outcome: Users experience smoother, buffer-free streaming and quicker downloads, enhancing their mobile internet experience.

b. Internet of Things (IoT):

- Performance: 5G's low-power, high-density capabilities enable massive IoT connectivity and low-latency communication, improving IoT device performance.
- Outcome: IoT applications, such as smart cities and industrial IoT, benefit from reliable and real-time data exchange, leading to improved efficiency and automation.

c. Fixed Wireless Access (FWA):

- Performance: 5G FWA offers high-speed internet in areas lacking wired infrastructure, with low latency for online activities and video conferencing.
- Outcome: Rural and underserved areas gain access to high-quality broadband internet, bridging the digital divide.

d. Public Safety and Emergency Services:

- Performance: 5G networks provide reliable, high-speed communication, enabling first responders to share critical information and coordinate effectively.
- Outcome: Improved situational awareness and faster response times can save lives in emergency situations.

e. Smart Manufacturing:

- Performance: 5G's low latency and high reliability facilitate real-time control and monitoring of machinery and processes in smart factories.
- Outcome: Enhanced automation and predictive maintenance lead to increased productivity and reduced downtime.

f. Healthcare:

- Performance: 5G enables high-resolution video streaming for telemedicine and real-time monitoring of patients.
- Outcome: Improved access to healthcare services and remote patient care, especially in remote or underserved areas**.**

g. Autonomous Vehicles (Connected and Autonomous Vehicles - CAVs):

- Performance: 5G supports ultra-reliable, low-latency communication (URLLC) crucial for CAVs, ensuring safe and efficient transportation.
- Outcome: Safer roads, reduced accidents, and the potential for fully autonomous vehicles in the future.

h. Smart Agriculture:

- Performance: 5G enables the connectivity of sensors and autonomous machinery, improving precision farming.
- Outcome: Higher crop yields, reduced resource wastage, and sustainable agriculture practices.

i. Entertainment and Gaming:

- Performance: 5G enables low-latency cloud gaming services for high-quality gaming experiences on mobile devices.
- Outcome: Gamers can enjoy console-level gaming on the go, with minimal lag.

5. Future Trends and Challenges

Future trends in direct resonator antennas for 5G include advancements in compact, multi-band designs to accommodate diverse frequency bands. Challenges involve addressing integration issues small form factors and optimizing antenna performance for the evolving 5G standards.

5.1. Emerging trends in DRA technology:

- **Millimetre-Wave and 5G Applications:** DRAs were gaining popularity in millimetre-wave bands for 5G and other high-frequency applications due to their compact size, high gain, and suitability for these frequency ranges.
- **Multiband and Wideband DRAs:** Researchers were working on designs to create DRAs capable of operating across multiple frequency bands, making them versatile for various wireless communication standards.
- **Metamaterial Integration:** Integration of metamaterials with DRAs to enhance their performance, including improved bandwidth, gain, and radiation efficiency.
- **Circularly Polarized DRAs:** Development of circularly polarized DRAs for satellite communication, automotive radar, and other applications requiring polarization diversity. Compact and Miniaturized DRAs: Efforts to miniaturize DRAs for portable devices, IoT applications, and wearables while maintaining their efficiency and radiation characteristics.
- **Dielectric Material Advances:** Research into new dielectric materials with improved properties for DRAs, such as higher permittivity and lower losses, to further enhance their performance.
- **Beamforming and MIMO:** Integration of DRAs into multiple-input, multiple-output (MIMO) systems for beamforming and spatial diversity, especially in the context of 5G networks.
- **Antenna-on-Chip (AoC):** Exploring the integration of DRAs onto semiconductor chips for applications in integrated circuits, communication systems, and emerging technologies like IoT.
- **Energy Harvesting**: Investigating the use of DRAs for energy harvesting from ambient RF signals, enabling low-power and self-sustaining devices in remote or IoT applications.
- **Environmental Considerations:**

  Developing DRAs with improved resistance to environmental factors, such as temperature extremes and moisture, for outdoor and rugged applications.
- **Advanced Fabrication Techniques:** Advancements in manufacturing methods, such as 3D printing and additive manufacturing, for producing customized and complex DRA designs.
- **AI-Driven Design:** Utilizing artificial intelligence and machine learning algorithms to optimize and automate the design of DRAs for specific performance requirements and frequency bands.
- **Satellite Communication:** DRAs were being explored for use in satellite communication systems due to their potential advantages in terms of size, weight, and performance.

6. Conclusion

In conclusion, electric resonator antennas show promise in 5G applications, offering compact designs and potential for millimetre-wave frequencies. However, addressing integration challenges and ensuring compatibility with evolving 5G standards are essential for their successful deployment.

Enhanced Gain: Compared to conventional antennas, the DRA exhibits significantly higher gain, making it ideal for long-range communication and signal coverage improvement.

Broader Bandwidth: The DRA covers a wider frequency range encompassing relevant 5G bands, offering flexibility for diverse applications.

Compact Design: The DRA maintains a compact size, making it suitable for integration into portable devices and space-constrained environments.

Tuneable Characteristics: The DRA's properties can be readily adjusted by manipulating the dielectric material and geometric parameters, allowing for customization to specific needs.

These advantages position the DRA as a viable candidate for 5G communication systems, particularly in scenarios requiring high gain, wide bandwidth, and compact form factors. Further research and development efforts can focus on optimizing the DRA design for specific 5G bands, exploring advanced materials with enhanced dielectric properties, and investigating integration techniques for practical applications.

- We can mention the specific gain and bandwidth improvement achieved compared to reference antennas.
- Briefly highlight the advantages of DRA over other antenna types for 5G applications.
- If your research involved simulations or experimental validation, summarize the key findings and their significance.
- Conclude by reiterating the potential of DRA for 5G communication and outlining future research directions.

A high-gain and wideband dielectric resonator antenna was designed, simulated, fabricated, and experimentally verified. The proposed structure achieved a wide bandwidth and high gain operating in higher-order mode using a new approach of putting a cylindrical hole at the center of the DRA. The DRAs were designed at the operating frequency of 15 GHz. The DRAs were fabricated and measured to validate the proposed design concept. Measured results of the fabricated antenna prototypes showed an impedance bandwidth of 10.7% from 14.3-15.9GHz and 16.1% from 14.1-16.5GHz with a high gain of 10.4dBi for DRA1 and DRA2, respectively. The measured and simulated results of the DRA were in good agreement. Furthermore, the results show that the designed antenna is suitable for future 5G communication applications.

Reference

[1] Fakhte, S.; Oraizi, H. Compact uniaxial anisotropic dielectric resonator antenna operating at higher order radiating mode. Electron.Lett. 2016, 52, 1579–1580.

[2] Sharma, A.; Biswas, A. Wideband multiple-input–multiple-output dielectric resonator antenna. IET Microw. Antennas Propag.2017, 11, 496–502.

[3] Sarkar, G.A.; Ballav, S.; Chatterjee, A.; Ranjit, S.; Parui, S.K. Four element MIMO DRA with high isolation for WLAN applications.Prog. Electromagn. Res. Lett. 2019, 84, 99–106.

[4] Varshney, G.; Singh, R.; Pandey, V.S.; Yaduvanshi, R.S. Circularly polarized two-port MIMO dielectric resonator antenna. Prog.Electromagn. Res. M 2020, 91, 19–28.

[5] Daghari, M.; Essid, C.; Sakli, H. Muli-UWB Antenna System Design for 5G Wireless Applications with Diversity. Wirel. Commun.Mob. Comput. 2021, 2021, 9966581.

[6] Roshani, S.; Yahya, S.I.; Alameri, B.M.; Mezaal, Y.S.; Liu, L.W.; Roshani, S. Filtering Power Divider Design Using Resonant LC Branches for 5G Low-Band Applications. Sustainability 2022, 14, 12291.

[7] Ali, A.; Tong, J.; Iqbal, J.; Illahi, U.; Rauf, A.; Rehman, S.U.; Ali, H.; Qadir, M.M.; Khan, M.A.; Ghoniem, R.M. Mutual Coupling Reduction through Defected Ground Structure in Circularly Polarized, Dielectric Resonator-Based MIMO Antennas for Sub-6GHz 5G Applications. Micromachines 2022, 13, 1082.

[8] Iqbal, A.; Nasir, J.; Qureshi, M.B.; Khan, A.A.; Rehman, J.U.; Rahman, H.U.; Fayyaz, M.A.; Nawaz, R. A CPW fed quad-port MIMO DRA for sub-6 GHz 5G applications. PLoS ONE 2022, 17, e0268867.

[9] Zhu, J.; Yang, Y.; Li, S.; Liao, S.; Xue, Q. Dual-Band Dual Circularly Polarized Antenna Array Using FSS-Integrated Polarization Rotation, A.M.C. Ground for Vehicle Satellite Communications. IEEE Trans. Veh. Technol. 2019, 68, 10742–10751.Upadhyaya, T.; Park, I.; Pandey, R.; Patel, U.; Pandya, K.; Desai, A.; Pabari, J.; Byun, G.; Kosta, Y. Aperture-Fed Quad-Port Dual-Band Dielectric Resonator-MIMO Antenna for Sub-6 GHz 5G and WLAN Application. Int. J. Antennas Propag. 2022, 2022,4136347.

[10] Ramos, A.; Varum, T.; Matos, J.N. Compact Multilayer Yagi-Uda Based Antenna for IoT/5G Sensors. Sensors 2018, 18, 2914. [Google Scholar] [CrossRef] [PubMed][Green Version]

[11] Bengtsson, E.L.; Rusek, F.; Malkowsky, S.; Tufvesson, F.; Karlsson, P.C.; Edfors, O. A Simulation Framework for Multiple-Antenna Terminals in 5G Massive MIMO Systems. IEEE

Access 2017, 5, 26819–26831. [Google Scholar] [CrossRef]

[12]Rahman, M.M.; Islam, M.S.; Wong, H.Y.; Alam, T.; Islam, M.T. Performance Analysis of a Defected Ground-Structured Antenna Loaded with Stub-Slot for 5G Communication. Sensors 2019, 19, 2634. [Google Scholar] [CrossRef] [PubMed][Green Version]

[13]Rappaport, T.S.; Xing, Y.; MacCartney, G.R.; Molisch, A.F.; Mellios, E.; Zhang, J. Overview of Millimeter Wave Communications for Fifth-Generation (5G) Wireless Networks-With a Focus on Propagation Models. IEEE Trans. Antennas Propag. 2017, 65, 6213–6230. [Google Scholar] [CrossRef]

[14]Feng, W.; Li, Y.; Jin, D.; Su, L.; Chen, S. Millimetre-wave backhaul for 5G networks: Challenges and solutions. Sensors 2016, 16, 892. [Google Scholar] [CrossRef]

[15]Ali, I.; Jamaluddin, M.H.; Kamarudin, M.R.; Gaya, A.; Dahri, M.H. Gain enhancement of dielectric resonator antenna for millimeter wave applications. TELKOMNIKA Telecommun. Comput. Electron. Control 2019, 17, 1670–1673. [Google Scholar] [CrossRef]

[16]Perron, A.; Denidni, T.A.; Sebak, A.R. High-Gain Hybrid Dielectric Resonator Antenna for Millimeter-Wave Applications: Design and Implementation. IEEE Trans. Antennas Propag. 2009, 57, 2882–2892. [Google Scholar] [CrossRef]

[17]Garg, R.; Bhartia, P.; Ittipiboon, A. Microstrip Antenna Design Handbook; Arteck House: Boston, MA, USA, 2001. [Google Scholar]

[18]James, J.R.; Hajj, P.S. Handbook of Microstrip Antennas; peter peregrinus Ltd. London United Kingdom: Oxford, UK, 1989. [Google Scholar]

[19]Itoh, T. Overview of Quasi-Planar Transmission Lines. IEEE Trans. Microwave Theory Tech. 1989, 37, 275–280. [Google Scholar] [CrossRef]

[20]Denldni, T.A.; Rao, Q.; Sebak, A.R. Two-ring slot-fed dielectric resonator antenna for dual-frequency operation. Microwave Opt. Technol. Lett. 2005, 44, 448–451. [Google Scholar] [CrossRef]

[21]Nasir, J.; Jamaluddin, M.H.; Ahmad, K.A.; Kamarudin, M.; Chee, Y.B.; Owais, O. Throughput measurement of a dual-band MIMO rectangular dielectric resonator antenna for LTE applications. Sensors 2017, 17, 148. [Google Scholar] [CrossRef][Green Version]

[22]Long, S.A.; McAllister, M.W.; Shen, L.C. The Resonant Cylindrical Dielectric Cavity Antenna. IEEE Trans. Antennas Propag. 1983, 31, 406–412. [Google Scholar] [CrossRef]

[23]Petosa, A. Dielectric Resonator Antenna Handbook; Artech House Publishers: London, UK, 2007. [Google Scholar]

[24]Shahadan, N.H.; Jamaluddin, M.H. Steerable Higher Order Mode Dielectric Resonator Antenna With Parasitic Elements for 5G Applications. IEEE Access 2017, 5, 22234–22243. [Google Scholar] [CrossRef][Green Version]

[25]Luk, K.M.; Leung, K.W. Dielectric Resonator Antennas; Research Studies Press: Hertfordshire, UK, 2003. [Google Scholar]

[26]Altaf, A.; Munkyo, S. Triple-Band Dual-Sense Circularly Polarized Hybrid Dielectric Resonator Antenna. Sensors 2018, 18, 3899. [Google Scholar] [CrossRef] [PubMed][Green Version]

[27]Denidni, T.A.; Weng, Z. Rectangular dielectric resonator antenna for ultrawideband applications. IEEE Trans. Antennas Propag. 2010, 58, 4059–4062. [Google Scholar] [CrossRef]

[28]Leung, K.W.; Wong, W.C.; Ng, H.K. Circularly polarized slot-coupled dielectric resonator antenna with a parasitic patch. IEEE Antennas Wirel. Propag. Lett. 2002, 1, 57–59. [Google Scholar] [CrossRef]

[29]Ryu, K.S.; Kishk, A.A. UWB dielectric resonator antenna having consistent omnidirectional pattern and low cross-polarization characteristics. IEEE Trans. Antennas Propag. 2011, 59, 1403–1408. [Google Scholar] [CrossRef]

[30]Chair, R.; Kishk, A.A.; Lee, K.F. Wideband stair-shaped dielectric resonator antennas. IET Microwaves Antennas Propag. 2007, 1, 299–305. [Google Scholar] [CrossRef]

[31]Kishk, A.A. Directive Yagi-Uda dielectric resonator antennas. Microwave Opt. Technol. Lett. 2005, 44, 451–453. [Google Scholar] [CrossRef]

[32]Hwang, Y.; Zhang, Y.P.; Luk, K.M.; Yung, E.K.N. Gain-enhanced miniaturised rectangular dielectric resonator antenna. Electron. Lett. 1997, 33, 350–352. [Google Scholar] [CrossRef]

[33]Cicchetti, R.; Faraone, A.; Miozzi, E.; Ravanelli, R.; Testa, O. A High-Gain Mushroom-Shaped Dielectric Resonator Antenna for Wideband Wireless Applications. IEEE Trans. Antennas Propag. 2016, 64, 2848–2861. [Google Scholar] [CrossRef]

[34]Esselle, N.K.P. Antennas with dielectric resonators and surface mounted short horns for high gain and large bandwidth. IET Microwave Antennas Propag. 2007, 1, 723–728. [Google Scholar]

[35]Fakhte, S.; Oraizi, H.; Matekovits, L. Gain Improvement of Rectangular Dielectric Resonator Antenna by Engraving Grooves on Its Side Walls. IEEE Antennas Wirel. Propag. Lett. 2017, 16, 2167–2170. [Google Scholar] [CrossRef]

[36]Guha, D.; Banerjee, A.; Kumar, C.; Antar, Y.M.M. New technique to excite higher-order radiating mode in a cylindrical dielectric resonator antenna. IEEE Antennas Wirel. Propag. Lett. 2014, 13, 15–18. [Google Scholar] [CrossRef]

[37]Guha, D.; Banerjee, A.; Kumar, C.; Antar, Y.M.M. Higher order mode excitation for high-gain broadside radiation from cylindrical dielectric resonator antennas. IEEE Trans. Antennas Propag. 2012, 60, 71–77. [Google Scholar] [CrossRef]

[38]Mongia, R.K.; Ittipiboon, A. Theoretical and experimental investigations on rectangular dielectric resonator antennas. IEEE Trans. Antennas Propag. 1997, 45, 1348–1356. [Google Scholar] [CrossRef]

[39]Mongia, R.K.; Bhartia, P. Dielectric resonator antennas—A Review and General Design Relation for Resonant Frequency and Bandwidth. Int. J. Microwave Millim. Wave Comput. Eng. 1994, 4, 230–247. [Google Scholar] [CrossRef]

[40]Pan, Y.M.; Leung, K.W.; Luk, K.M. Design of the millimeter-wave rectangular dielectric resonator antenna using a higher-order mode. IEEE Trans. Antennas Propag. 2011, 59, 2780–2788. [Google Scholar] [CrossRef]

[41]Li, C.H.; Chiu, T.Y. 340-GHz Low-Cost and High-Gain On-Chip Higher Order Mode Dielectric Resonator Antenna for THz Applications. IEEE Trans. Terahertz Sci.Technol. 2017, 7, 284–294. [Google Scholar] [CrossRef]

[42] Hou, D.; Hong, W.; Goh, W.L.; Chen, J.; Xiong, Y.Z.; Hu, S. D-band on-chip higher-order-mode dielectric-resonator antennas fed by half-mode cavity in CMOS technology. IEEE Antennas Propag. Mag. 2014, 56, 80–89. [Google Scholar] [CrossRef]